Journal of Building Technology, 2024, Volume 6, Issue 2
DOI: 10.32629/jbt.v6i2.2545
ISSN Online: 2717-5103
ISSN Print: 2705-1390

Seismic-resistant Design Regulations for Structures, Earthquake and Experimental Results Lessons

Mario E. Rodriguez

Instituto de Ingeniería, UNAM, Ciudad Universitaria, Ciudad de México, CP 04510, México.

Abstract: The Mexico City earthquakes of September 19, 1985, and September 19, 2017, showed that the seismic requirements for these earthquakes exceeded those specified in the Mexico City building code. This study illustrates limitations in current procedures for the seismic analysis of structures. The uncertainties in the assessment of seismic design requirements and limitations in the seismic analysis of structural systems indicate that the lateral strength specified in building codes is not sufficient and that structures must have lateral deformation capacity. It follows that structural systems with low or intermediate ductility, such as those allowed in the Mexico City Building Code (MCBC, 2017), would not be desirable for resisting strong earthquakes. The last part of this work shows computed story drifts in buildings with different structural systems, either based on frames or using structural walls. This study compares story drifts in these structural systems for both using the seismic demands specified by MCBC 2017 and for the seismic demands corresponding to the September 19, 2017, earthquake in Mexico City. The results for these story drifts show the importance of rigid structural systems for reducing story drift demands, not only for avoiding collapse in strong earthquakes but also for significantly reducing building damage.

Key words: seismic design; seismic building codes; earthquakes; story drift; experimental results

1. Introduction

Some authors have mentioned that in engineering problems, there are two criteria for their solution, which sometimes confront each other without reaching a consensus. These criteria are theoretical and observational. This work carries out a critical evaluation of some aspects of seismic-resistant design regulations of structures, taking into account observations in past earthquakes, as well as considering some limitations of seismic analysis procedures of structures, and limitations identified based on the observation of mainly experimental results. The uncertainty of the values of the design seismic actions, and the limitations of seismic analysis procedures of structures, suggest that it is not enough for the structures to have the lateral resistance specified by standards, and that it is necessary for the structures to have reserves of deformation capacity.

This study also shows the importance of using rigid structures to reduce the demands of interstory distortions in buildings, in order to not only avoid collapse in strong earthquakes, but also to reduce damage to structures in these earthquakes.

2. Uncertainties Observed in the Seismic Design Demands Specified by Regulations in Various Countries

Observations of past earthquakes in Mexico and around the world indicate significant differences between the seismic demands observed in some earthquakes and the design requirements specified by current regulations at the time of these events. Rodriguez (2016) provided detailed evidence for the Mexico City earthquake on September 19, 1985, the Chile earthquake on February 27, 2010, and the New Zealand earthquakes on September 4, 2010 and February 22, 2011. The following is a summary of the evidence and adds relevant observations discovered during the Mexico City earthquake on September 19, 2017, as demonstrated by this study, which provide useful lessons for seismic design practices.

2.1 The Mexico City earthquake of September 19, 1985

The earthquake of September 19, 1985 with epicenter in the coast of Michoacán, caused collapses or severe damages in hundreds of buildings in Mexico City. Rodriguez (2016) describes some characteristics of these damages. In the area of greatest damage, the acceleration record was obtained from the SCT station, which has been widely used in studies with analytical models of seismic response prediction.

Fig. 1 (Rodriguez, 2016) shows acceleration spectra that were computed for the acceleration record obtained at the SCT station, specifically the horizontal component EW, using a percentage of critical damping equal to 5%. Fig. 1 also depicts the acceleration spectra obtained using the specifications of the regulations in force at the time of the earthquake, namely the Building Regulations for the Federal District of 1976 (RCDF, 1976). For these spectra, the specified spectral ordinates were multiplied by an over-resistance factor for structures, which, in this study, was deemed equal to 2. It can be observed that within a time period ranging from approximately 1.5 s to 2.8 s, the elastic spectral ordinates calculated for the SCT record in its EW component are greater than those that would be derived from the specifications of the RCDF 1976, with the largest discrepancy occurring for values of T, the fundamental period of buildings, that are close to 2 s.

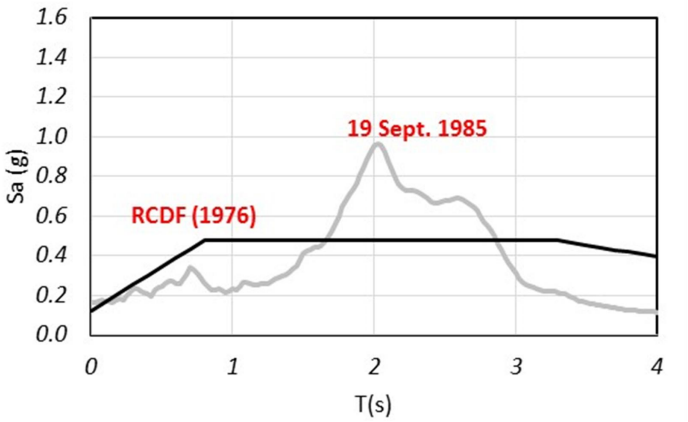

Figure 1. Spectral accelerations obtained with the acceleration record of the Mexico 1985 earthquake at the SCT station and transparent design spectrum of Mexico City 1976 (Rodriguez, 2016).

2.2 Maule Earthquake, in Concepción, Chile, February 27, 2010, $M = 8.8$

Concepción was the city in Chile where the greatest damage to buildings occurred in the earthquake of February 27, 2010. Structural damage was observed in about 10% of buildings with more than 10 floors in Concepción (Massone et al., 2012). This study uses acceleration records from the Concepción Centro station, located in the area of the city where the damage to buildings was concentrated. These records correspond to the horizontal components L and T. The Concepción Centro station is located in sandy soil, and because of the shear wave velocity at the site, $V_s = 230$ m/s, it would be classified as type D according to the ASCE 7-16 classification (ASCE 7-16, 2016).

Fig. 2 (Rodriguez, 2016) shows the elastic acceleration spectra for the selected records of the Concepción Centro station, in their two horizontal components, which were calculated with a percentage of the critical damping equal to 5%. Fig. 2 also shows, with continuous black lines, the elastic design spectra specified by the seismic design standard in force at the date of the earthquake, NCh 433 (NCh 4333, 1996), for soils classified by that standard as soil types III and IV. The area of greatest structural damage in Concepción was classified as soil type III.

Results of Fig. 2 show that the elastic spectral ordinates calculated for the records of the Concepción Centro station, in their horizontal components L and T, are much higher than those specified by the local standards for Type III soils, in the structural period zone in the interval from about 1.5 s to 3 s. Fig. 2 shows that in the period interval between about 1.5 s to 2.5 s, the spectral ordinates of the Concepción Centro station records exceeded even the values specified by the NCH 433 standard for Type IV soil structures. Due to this experience in the Maule earthquake, the seismic design regulations in Chile in 2011 changed the seismic classification of the terrain, adding two more soil types (Diario Oficial, 2011).

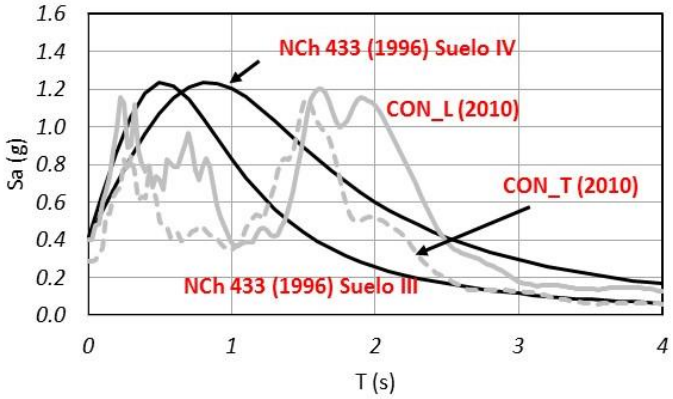

Figure 2. Horizontal spectral accelerations obtained with acceleration records from the Concepción Centro station in the Maule earthquake, Chile 2011, and accelerations specified by the Chilean Standard of 1996 (Rodriguez, 2016).

2.3 Earthquakes in Christchurch, New Zealand, in 2010 and 2011

On February 22, 2011, an earthquake affected the city of Christchurch, New Zealand, and the epicenter was practically located in the city and its magnitude was *Mw* = 6.2. This earthquake can be considered as an aftershock of the earthquake that occurred on September 4, 2010, with epicenter at a distance of about 40 km from the city, and with *Mw* = 7.1 (Bradley et al., 2014). The 2011 earthquake caused significant collapse and damage to residential and commercial buildings, houses, bridges, and vital subway lines, as well as 185 fatalities. For this study, records obtained at the Christchurch Cathedral College (CCC) station, located in the area of greatest damage in the city, were selected. The station is located in soil type D, soft or deep soils, of the soil classification specified in the New Zealand Loading Standard (NZLS, 2004).

Fig. 3 (Rodriguez, 2016) shows elastic acceleration spectra for the CCC station for the 2010 and 2011 earthquakes, with black and gray lines, respectively, in their two horizontal components. These spectra were calculated with a percentage of the critical damping equal to 5%. Additionally, Fig. 3 displays the elastic design spectra specified by NZLS (2004) for this part of the city, depicted by continuous black lines. These include both the spectrum corresponding to the 500-year return period and the spectrum corresponding to the 2500-year return period (EERI, 2011). The results in Fig. 3 show that the calculated elastic spectral ordinates for the 2011 earthquake are quite larger than those of the 2010 earthquake in the zone of periods less than 1.5 s. For periods shorter than 2 s, the spectral ordinates of records obtained in the 2010 earthquake are close to the ordinates specified by NZLS (2004) for the earthquake with a 500-year return period, while, for this period interval, the spectral ordinates of records obtained in the 2011 earthquake are close to or even larger

than the ordinates specified by NZLS (2004) for the earthquake with a 2,500-year return period. These results show that earthquakes whose return periods, according to NZLS (2004), were estimated at 500 and 2,500 years occurred in less than one year, which is an evident sign of the existing uncertainties in the definition of seismic design demands.

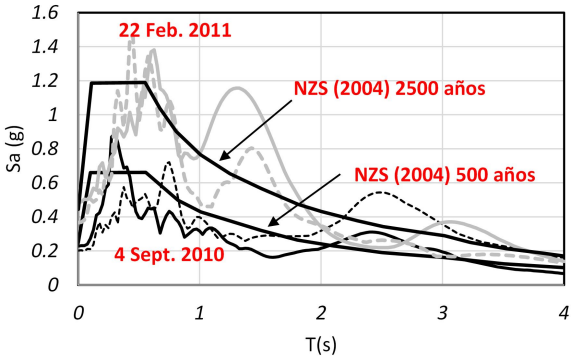

Figure 3. Horizontal spectral accelerations obtained with acceleration records from the CCC station in the Christchurch 2010 and 2011 earthquakes, and accelerations specified by NZLS (2004) (Rodriguez, 2016).

2.4 Earthquake of September 19, 2017 in Mexico City

On September 19, 2017, an M 7.1 earthquake occurred in Mexico of the intraplate type, with an epicenter in the State of Morelos, about 120 km from Mexico City. The earthquake caused the collapse of approximately 50 buildings in the CDMX, a number estimated according to data obtained by structural engineers organized by technical societies such as the Mexican Society of Structural Engineering (SMIE) and was coordinated by the College of Civil Engineers of Mexico (CICM). These engineers inspected most of the damage to buildings in Mexico City due to this earthquake. Rodriguez (2020) describes some of the characteristics of building damage observed in this earthquake.

Fig. 4 shows, with continuous lines, the spectra of accelerations and elastic displacements, respectively depicted in Figs. 4(a) and 4(b), which were calculated for the records obtained at the SCT station during the September 19, 1985, and 2017 earthquakes. Fig. 4 demonstrates that, in the period zone shorter than 1.8 s, the demands of both seismic events are comparable. Additionally, Fig. 4 also displays, with a dotted line, the elastic spectrum obtained using SASID, which is a component of the Complementary Technical Standards for Earthquake Design of Mexico City (NTCS, 2017). In general, this spectrum has higher spectral ordinates than those derived from the records of both earthquakes. Virtually all of the buildings that collapsed in 2017 had previously withstood the 1985 earthquake without any evidence of significant damage. This characteristic, along with the similarities in seismic demands observed at the SCT station during a specific period in both the 1985 and 2017 earthquakes, suggests the presence of accumulated damage in structures that endure multiple earthquakes, as analyzed by Rodriguez (2020).

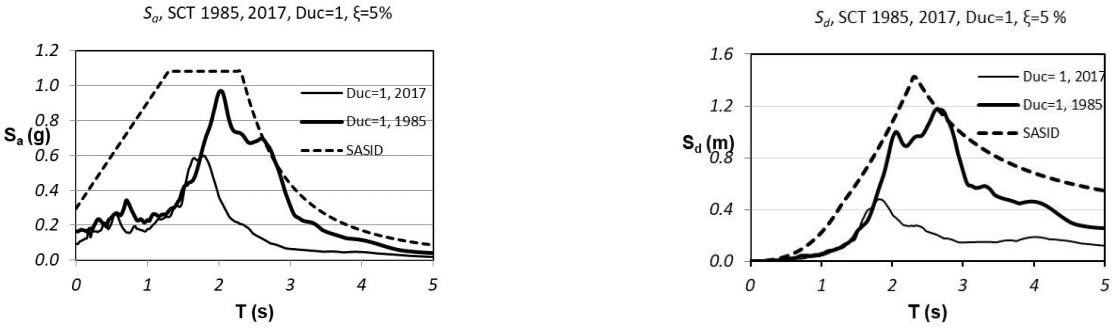

(a) Acceleration spectrum (b) Displacement spectrum

Figure 4. Accelerations and elastic horizontal spectral displacements obtained at station SCT with acceleration records from the September 19, 1985 and 2017 earthquakes, and elastic spectra obtained with SASID.

This paper uses acceleration records obtained at the Miramontes station in the earthquake of September 19, 2017. This station is located in the south of Mexico City, started to operate after the occurrence of the earthquake of September 19, 1985, and is quite far from the area where most of the building collapses occurred in Mexico City in that seismic event. Most of the damage and collapses observed in buildings in Mexico City in the September 19, 2017 earthquake occurred in buildings located on soils with similar values of dominant ground periods, *Ts*, ranging from 1 s to 1.5 s (Rodriguez, 2020). This interval coincides with the dominant ground period of the Miramontes station. Fig. 5 shows, with a thin continuous line, the spectra of accelerations and elastic displacements obtained for the S00E record of this station in the 2017 earthquake. The thick solid line in Fig. 5 shows the elastic spectral design ordinates in the area of the station, classified as soft soil, Zone IIIa, according to NTCS (2004), which was in force at the time of the aforementioned earthquake. These ordinates were obtained by multiplying the spectral ordinates specified in the NTCS (2004) by the structural over-resistance factor, which was considered equal to 2. The results in Fig. 5 show that in a zone of periods approximately between 1.2 s and 1.6 s, the elastic spectral design ordinates specified by the NTCS (2004) underestimate the demands computed using the accelerations recorded at the Miramontes station. Moreover, these latter demands exceed, in that same period interval, the design demands of NTCS 2017 (NTCS, 2017) and SASID, which are shown with dashed lines in Fig. 5.

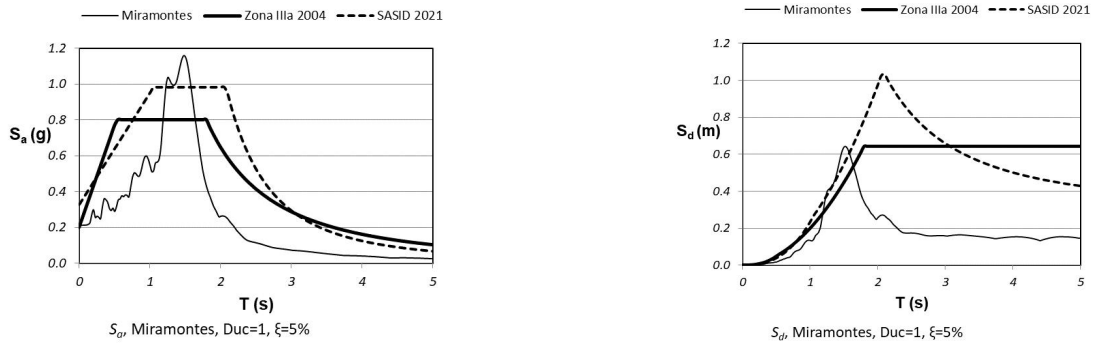

(a) Acceleration spectrum (b) Displacement spectrum

Figure 5. Horizontal spectral accelerations and displacements in the elastic interval obtained at the Miramontes station with accelerations record of the September 19, 2017 earthquake, and elastic spectra obtained with the standard for Mexico City 2004 and with SASID.

The dashed lines shown in Fig. 6, labeled as SASID, $Q = 2$ and SASID, $Q = 4$, were derived from the unreduced elastic spectral accelerations specified in the NTCS 2017 standard (NTCS, 2017) and SASID for the Miramontes station site. These values were then divided by the corresponding seismic behavior reduction factor, Q', for the cases where the seismic behavior factor, Q, is equal to 2 and 4.Fig. 6 also shows, with continuous lines, the spectral accelerations obtained from the nonlinear analysis of a 1GDL oscillator when responding to the S00E accelerations record obtained at the Miramontes station in the earthquake of September 17, 2017, considering the values of displacement ductility, μ, equal to 2 and 4, thick and thin lines, respectively, for $\xi = 5$ %. These results indicate that in certain period intervals the observed seismic demands in the referred earthquake were higher than the stipulated ones. For example, for the case of $\mu = 2$, approximately this period interval was from 0.9 s to 1.3 s, and for the case $\mu = 4$, the interval was from 0.3 s to 1.1 s, see Fig 6.

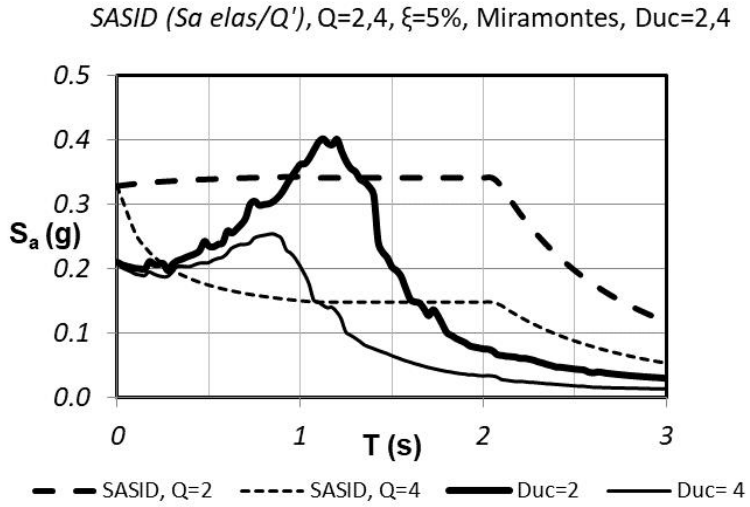

Figure 6. Spectral accelerations in the inelastic interval obtained with the S00E accelerations record of the September 19, 2017 earthquake at Miramontes station for the ductility cases of displacements equal to 2 and 4, and design spectra obtained with NTCS 2017 and with SASID for the cases $Q = 2$ and $Q = 4$.

These results present a unique case where the seismic demands observed during the earthquake at the Miramontes station surpassed those specified in the NTCS 2017 (NTCS, 2017) and SASID regulations for the station's location, even though these regulations had not yet been officially approved at the time. The seismic event under study occurred in September 2017 and the aforementioned regulation was published in December 2017. This can also be interpreted as follows: If the seismic demands observed during the mentioned seismic event surpassed those stipulated by the NTCS 2017, which were based on a low probability of occurrence within a certain return period, such as 250 years, then in reality, this probability was effectively 1, even prior to the official publication of the regulation.

This study shows that the seismic demands observed in the earthquakes in the world selected for this research, in all cases exceeded the demands stipulated by construction regulations in the respective places of occurrence of the earthquakes, showing the limitations of the probabilistic models used to define the seismic hazard and the consequent design earthquake. This evidence has several implications for existing or future seismic-resistant standards to be proposed in Mexico. One of these implications is to recognize the high probability of a seismic event exceeding the design demands. Additional important implications are discussed later in this article.

3. Uncertainties in Seismic Analysis Models of Structures

The application of seismic design standards requires the use of seismic analysis models of structures. In the subsequent discussion, uncertainties inherent in these models will be addressed, particularly those pertaining to the values adopted for the modulus of elasticity of concrete and the moments of inertia of structural elements. These properties significantly impact the natural vibration periods of the structure, and consequently, its seismic response. Additionally, uncertainties that exist in the computation of the seismic response of irregular structures are discussed, as well as limitations of the conventional modal analysis are shown.

3.1 Variability of the modulus of elasticity of concrete

The modulus of elasticity of concrete is a relevant parameter in the computation of seismic demands in structures, since it plays an important role in the lateral stiffness of a structure, and therefore in its vibration periods, directly related to the values of seismic demands specified in the design spectra. This suggests the need to evaluate the results of existing procedures in standards for the computation of the modulus of elasticity of concrete and to compare these results with experimental results.

The Complementary Technical Standards for Design and Construction of Concrete Structures for Mexico City (NTCC, 2017) stipulates for structural concretes or class I:

For low strength concretes (fc' < 40 MPa):

$$E_c = 4400\sqrt{f_c'}\ , E_c\ y\ f_c'\ en\ MPa \tag{1}$$

For high strength concrete (40 MPa < fc'< 70 MPa).

$$E_c = 2700\sqrt{f_c'} + 11000\ , \quad E_c\ y\ f_c'\ en\ MPa \tag{2}$$

The American Concrete Institute Committee ACI-363 (ACI-363, 1992) proposed the following expression for the estimation of the elastic modulus of concrete in the United States:

$$E_c = 3320\sqrt{f_c'} + 6900\ , \quad E_c\ y\ f_c'\ en\ MPa \tag{3}$$

American Concrete Institute Committee ACI 318 ACI-318-19 (ACI-318, 2019) states:

$$E_c = 0.043\, w_c^{1.5}\sqrt{f_c'}\ , \quad E_c\ y\ f_c'\ en\ MPa,\ \mathrm{w_c\ en\ kg/m^3} \tag{4}$$

For normal weight concrete, ACI 318-19 specifies:

$$E_c = 4700\sqrt{f_c'}\ , E_c\ y\ f_c'\ en\ MPa \tag{5}$$

Rodelo et al. (2020) obtained values of the modulus of elasticity of concrete in tests of concrete cylinders produced in different states of Mexico, the results of which are described in the following. Fig. 7 shows these results, as well as the values that would be obtained with the mentioned procedures of NTCC 2017, ACI 363, and with Eq. (4) of ACI 318-19. The results show that NTCC 2017, in most of the cases studied, underestimates the values of the modulus of elasticity of concrete for various regions of the country, particularly for concretes produced in Chihuahua and Monterrey. This difference was actually to be expected, since the NTCC 2017 expressions for *Ec*, are for concretes with aggregates used in the CDMX, which are not necessarily similar to those of other regions of the country. The mean and CV between the measured and calculated values for the Rodelo et al. (2020) database, with the NTCC 2017 expressions for *Ec* were equal to 1.11 and 0.17, respectively. For the case of using Eq. (4) of ACI 318-19, the mean and CV were equal to 1.02 and 0.19, respectively.

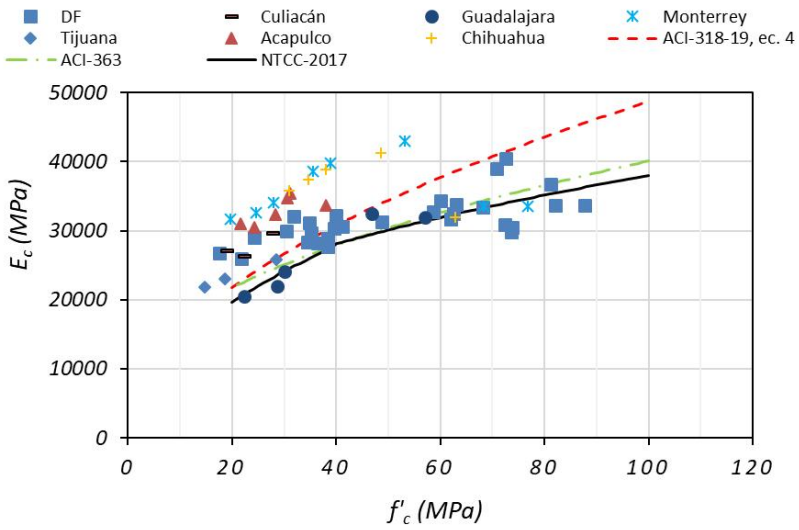

Figure 7. Results of *Ec* values measured and calculated with different procedures (Rodelo et al., 2020).

Rodelo et al. (2020) proposed the following expression for the computation of *Ec*:

$$E_c = 0.14\, w_c^{1.5} \left(f_c'\right)^{0.18}, \quad E_c \text{ y } f_c' \text{ en } MPa, \text{ w}_c \text{ en kg/m}^3$$

$$\left(E_c = 0.94\, w_c^{1.5} \left(f_c'\right)^{0.18}, \quad E_c \text{ y } f_c' \text{ en } kg/cm^2, \text{ w}_c \text{ en kg/m}^3\right) \tag{6}$$

Fig. 8(a) shows results of the computation of *Ec* using Eq. (6) divided by the factor that considers the type of aggregate, $w_c^{1.5}$, as well as results of measurements of the modulus of elasticity in the tests carried out in Mexico, when the cases of Chihuahua and Monterrey are excluded. It can be seen that the prediction given by Eq. (6) is acceptable. Fig 8(b) shows results with the same experimental data, but adding the cases of Chihuahua and Monterrey. These results indicate that the type of aggregate in the latter regions is an important factor influencing the value of *Ec*, and should therefore be taken into account in the prediction of *Ec*.

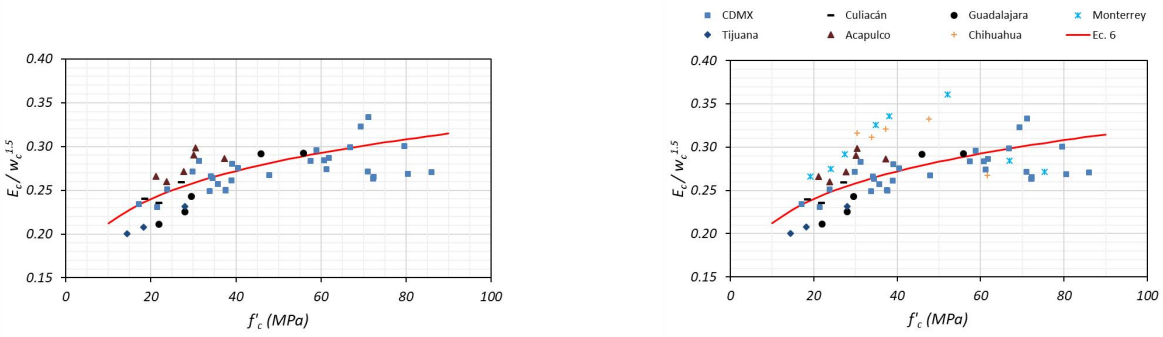

(a) Excluding data from Chihuahua and Monterey (b) Including all data

Figure 8. Measured and calculated values of $Ec/w_c^{1.5}$ using Eq. 6 (Rodelo et al., 2020).

When considering all the cases of the database of modulus of elasticity results obtained in concrete cylinder tests performed by Rodelo et al. (2020), the mean between the measured and calculated values with Eq. (6) was 1.01, and the CV value was equal to 0.11. These results indicate that the proposed expression, Eq. (6), leads to results with better statistical parameters than those previously discussed, corresponding to the case of using the expressions of the NTCC 2017, and Eq. (4) of the ACI 318-19. This characteristic of Eq. (6) suggests that this expression could be used at the national level.

3.2 Different definitions of stiffnesses in structural elements that influence the computation of distortions and vibration periods of buildings subjected to earthquakes

Several building codes specify values of effective moments of inertia, *Ie*, to be used in the seismic analysis of structures. For example, NTCC 2017 stipulates that for cracked reinforced concrete elements, the value 0.7*Ig* for columns and 0.5*Ig* for beams and walls, where *Ig* is the moment of inertia of the gross section. ACI 318-19 specifies that for lateral load analysis, the value of 0.5*Ig* should be used for *Ie* in structural elements.

Based on the use of experimental data, Elwood and Eberhard (2009) proposed the following expression for the effective lateral stiffness of reinforced concrete columns *EcIe*.

$$\frac{E_c I_e}{E_c I_g} = \frac{0.45 + 2.5 \dfrac{P}{A_g f'_c}}{1 + \dfrac{110}{\dfrac{h}{d_b}\dfrac{a_v}{h}}} \le 1.0 \quad y \ge 0.2 \tag{7}$$

Where P is the axial load acting on the column, Ag is the gross cross-sectional area of the column, d_b is the diameter of the longitudinal reinforcing bars, h is the column camber, and a_v is the shear span or length of a cantilever column. For the ratio h/d_b, these authors propose the values 25 and 18, for bridge and building columns, respectively.

Based on analytical and experimental studies, Restrepo and Rodriguez (2021) proposed the following expression for the effective lateral stiffness of reinforced concrete columns:

$$\frac{E_c I_e}{E_c I_g} = \left(\zeta'_{AR} + \zeta'_P\right)\zeta'_s \tag{8}$$

Where:

$$\zeta'_{AR} = \frac{\min\left(\mathrm{a_v}/\mathrm{h}, 6\right)}{14} \tag{9}$$

$$\zeta'_P = \frac{\dfrac{P}{A_g f'_c}\,\dfrac{\mathrm{f'_c}}{42\mathrm{MPa}}}{0.55 + 1.2\dfrac{P}{A_g f'_c}\,\dfrac{f'_c}{42\mathrm{MPa}}} \tag{10}$$

$$\zeta'_s = 1 - \frac{1}{2.5}\left(1 - \frac{P}{A_g f'_c}\,\frac{f'_c}{42\mathrm{MPa}}\right)\left(\frac{5}{3}\,\frac{f_y}{693\mathrm{MPa}} - 1\right) \tag{11}$$

Where f_y is the yield stress of the longitudinal reinforcement.

Fig. 9 shows results of the application of Eq. (7) proposed by Elwood and Eberhard (2009), and Eq. (8) proposed by Restrepo and Rodriguez (2021), which are indicated with a thin red and a thick black solid line, respectively. The results are shown as a function of the ratio $P/(A_g f'_c)$, considering $h/d_b = 18$, $a_v/h=2$, $f'_c = 30$ MPa, and $f_y = 420$ MPa. Fig 10 shows results of the same type, but for the case at $v/h = 4$. In addition, Figs. 9 and 10 show, with dashed lines, the results of employing the value of the effective stiffness ratio $E_cI_e/E_cI_g = 0.5$ specified by ACI 318-19 for reinforced concrete columns, as well as the value of the effective stiffness ratio $E_cI_e/E_cI_g = 0.7$ specified by NTCC 2017 for columns. As Figs. 9 and 10 indicate, the results of the application of the criteria of these two standards are quite far from the effective stiffness predictions proposed by Elwood and Eberhard (2009), and Restrepo and Rodriguez (2021), which as mentioned have been validated with experimental results. .These results show that the NTCC 2017 criterion for defining effective stiffnesses leads to a significant overestimation of the effective stiffness of columns over a wide range of values of the axial load ratio $P/A_g f'_c$, particularly for typical v/h ratios found in buildings, as is the case for values of the v/h ratio less than 4.

$$\frac{E_c I_e}{E_c I_g} = 0.16 + \frac{P}{A_g\,\mathrm{f'_c}} \tag{12a}$$

The results of using Eq. (12a) are shown in Figs. 9 and 10 with a continuous gray line, where it can be seen that these results are between the values obtained with expressions (7) and (8), proposed by Elwood and Eberhard (2009), and Restrepo and Rodriguez (2021), respectively. These results suggest that, due to its simplicity, Eq. (12a) could be used in future regulations in Mexico. Restrepo and Rodriguez (2021) suggest that concretes with f'_c values greater than 42 MPa, increase the effective stiffness. For these cases, in order to obtain better predictions of the effective stiffness of columns, these authors suggest multiplying the factor $P/A_g f'_c$ by the factor $f'_c/42$ MPa, whereby for concretes with f'_c values greater than 42 MPa, eq (12a) becomes:

$$\frac{E_c I_e}{E_c I_g} = 0.16 + \frac{P}{A_g \, \mathrm{f}'_c} \, \frac{\mathrm{f}'_c}{42\,\mathrm{MPa}} \qquad (12b)$$

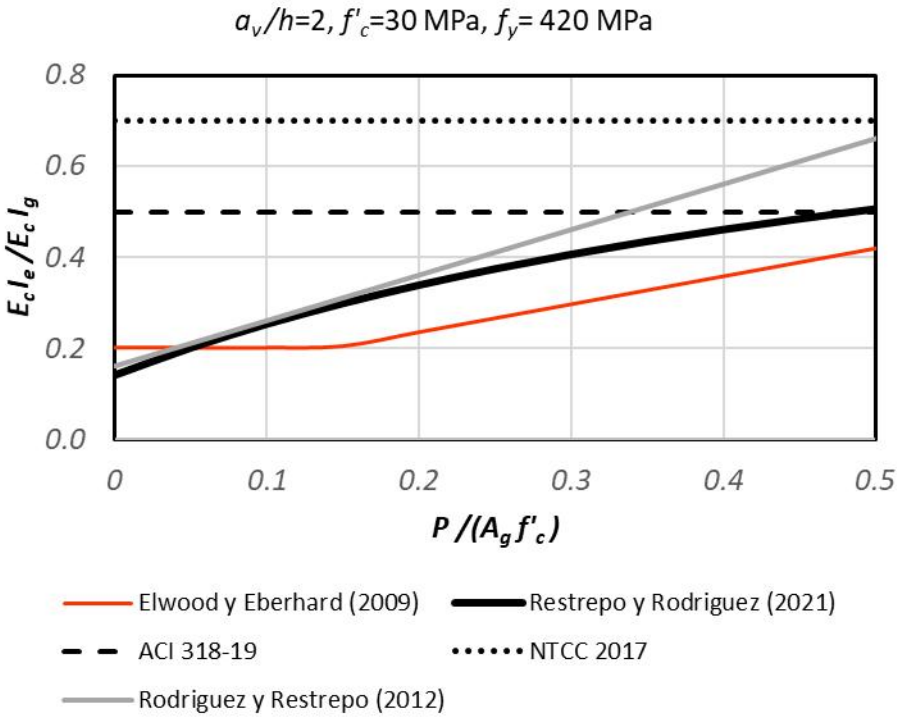

Figure 9. Results of the computation of effective stiffnesses using different criteria. Case a_v/h = 2.

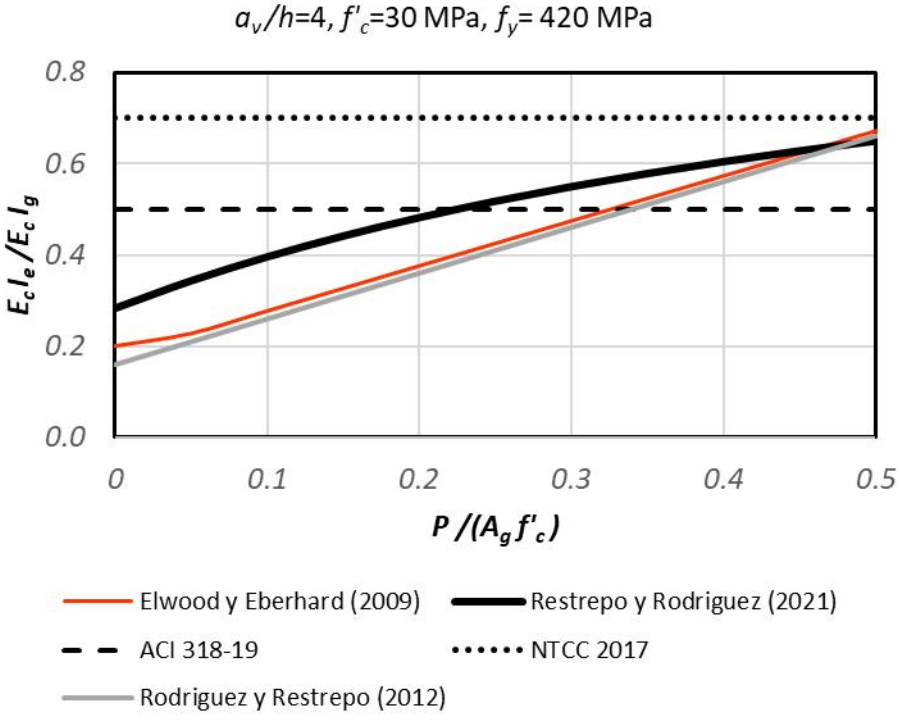

Figure 10. Results of the computation of effective stiffnesses using different criteria. Case a_v/h = 4.

The results presented in this study indicate that the application of the criteria stipulated by NTCC 2017 and ACI 318-19 to define effective stiffnesses would lead to seismic analysis results that do not adequately reflect the expected seismic behavior of buildings. This inadequacy is evident both in the prediction of distortions in the building prior to the design earthquake and in the prediction of the building's vibration periods, which are crucial factors in the computation of accelerations and displacements defined in the design spectra stipulated by the standards.

3.3 Limitations in conventional modal analysis

In several building regulations, including NTCS 2017, in seismic analysis the modal response S is obtained with the expression.

$$S = \sqrt{\sum S_i^2} \qquad (13)$$

Where S_i is the response in the i-th mode of the structure, which is obtained in the case of the NTCS 2017 with the value of the elastic response divided by $Q'R$. There is evidence that the modal response S may be underestimated if Eq. (13) is used, because the ductility in the structure does not reduce the effect of the higher modes, as it does for the case of the first mode (Rodriguez et al., 2002). This characteristic of the participation of the higher modes in the response of the structure is taken into account by ASCE 7-16 and NTCS 2017 in the seismic design of diaphragms in buildings, for the computation of the seismic forces acting in the plane of the diaphragms. The expressions stipulated by these standards for the computation of the horizontal accelerations acting on the diaphragms are obtained as the combination of the accelerations of the first mode reduced by ductility, combined with the accelerations of the higher modes without reduction by ductility.

This effect of different participation of the first and higher modes in the seismic response of a building is taken into account in other standards for the seismic shear design of special reinforced concrete structural walls, such as the New Zealand Standard 3101 (NZS 3101, 2006) and ACI 318-19 (ACI 318-19, 2019). NTCS 2017 or NTCC 2017 do not use this criterion for the seismic design of reinforced concrete structural walls.

3.4 Seismic analysis of irregular buildings

Irregular structures are characterized by amplified seismic demands on them, which cannot be reliably known with common elastic seismic analysis procedures used in practice (Shahrooz and Moehle, 1990). This implies that it is desirable to limit the use of irregular structures, and even prohibit them in areas of high seismicity and in important structures.

3.5 Comments

The uncertainties in the values of design seismic actions and in the results of seismic analysis models for structures, both of which are discussed with examples in this study, along with the amplification of seismic demands in irregular buildings and the influence of higher modes on the seismic response of structures, indicate that merely complying with the strength requirements of seismic design standards is insufficient. It is necessary for structures to possess reserves of deformation capacity. However, these reserves would not be achievable in structures designed with the seismic behavior factor Q = 2, a value commonly employed in Mexico. This is due to the low deformation capacity of their critical sections, primarily stemming from the limitations of transverse reinforcement typical in structures designed with Q = 2. It is crucial to consider the significance of transverse reinforcement in reinforced concrete elements in order to enhance the deformation capacity of the critical sections of structural elements exposed to earthquakes.

These results also highlight the importance of limiting the use of flexible structures, which cannot only lead to damage or collapse of so-called non-structural elements during intense or even moderate earthquakes, but also to collapses of these structures themselves, as occurred in the earthquake of September 19, 2017 in Mexico City. Typical examples of

this type of structure include those that utilize frame-based designs, a solution favored by architects in Mexico due to its lesser disruption of the spaces utilized in the architectural process, compared to the alternative of using reinforced concrete structural walls. The significance of the structural system in mitigating damage or preventing collapse of structures during earthquakes is discussed in the subsequent section of this paper.

4. The Importance of the Seismic-resistant Structural System to Limit Damage and Collapse in Earthquakes

In this section of the paper, we present the outcomes of employing approximate methods for calculating interstory distortions in reinforced concrete structures that are either primarily based on structural walls or a combination of frames and structural walls. These calculations are performed when these structures are subjected to typical acceleration records obtained during major earthquakes in Mexico City. The primary objective is to demonstrate the significant reduction in lateral displacements that can be achieved by utilizing structural walls, in comparison to a solution that relies solely on frames.

4.1 Approximate procedure for the computation of maximum distortions of floor-to-floor reinforced concrete structures

The procedure employed in this work for the computation of distortions in buildings is initially based on the computation of the maximum global distortion of a building, D_{rm}, a parameter defined as

$$D_{rm} = \frac{\delta_m}{H} \qquad (14)$$

Where δ_m is the maximum lateral displacement of the last floor of the building subjected to ground motion, and H the height of the building. The approximate analysis in this study employs the well-known concept of the equivalent structure, which is a 1GDL structure with the same period and displacement ductility as the building would have with various degrees of freedom (Saiidi and Sozen, 1981). For the record of accelerations under study, this system has the spectral displacement (maximum) equal to S_d. The displacement δ_m can be obtained with the product $\Gamma_{m1}S_d$, where Γ_{m1} is the participation factor of the first mode. For the computation of this parameter, the procedure specified by ASCE/SEI 7-16 (ASCE 7, 2016) for the computation of Γ_{m1} for seismic design purposes of diaphragms in n-story buildings is used in this work. This parameter is defined as:

$$\Gamma_{m1} = 1 + \frac{z_s}{2}\left(1 - \frac{1}{n}\right) \qquad (15)$$

Based on the above, the distortion D_{rm} is expressed as follows:

$$D_{rm} = \frac{\Gamma_{m1}\, S_d}{H} \qquad (16)$$

A simple approximate expression used for estimating the fundamental period, T, of a building is

$$T = \frac{n}{\lambda} \qquad (17)$$

Where λ is a factor that depends on the type of structural system of the building, and has units s^{-1}.

In a regular building, the height H can be expressed as a function of the mezzanine height, h, as:

$$H = n\, h \qquad (18)$$

The stiffness index H/T (Lagos et al., 2012; Rodriguez, 2018) is introduced, which from eqs. (17) and (18) is equal to

$$\frac{H}{T} = \lambda\, h \qquad (19)$$

Eq. (16) is expressed as a function of the stiffness ratio *H/T* as:

$$D_{rm} = \frac{\Gamma_{m1}\, S_d}{T\,(H/T)} \qquad (20)$$

In this study, the value of the floor-to-ceiling height h in the studied buildings is estimated to be equal to 3.5 m. For the case of reinforced concrete frames, in this study, $\lambda = 8\ s^{-1}$ is considered (Pujol and Rodriguez, 2019). The value of λ in buildings with reinforced concrete structural walls can vary in an important interval, depending on the density of walls, for example, the interval of 10 s^{-1} to 14 s^{-1} is suggested. For Chile, the average stiffness index *H/T* in reinforced concrete buildings with structural wall based structural systems is 50 m/s (Rodriguez, 2018), with a height of h = 3.5 m, as shown in Eq. (19) corresponds to an average value of 14 s^{-1} for λ, which is the upper limit of the parameter λ within the recommended range of reinforced concrete structural wall buildings for this project. This is due to the fact that the construction practice in Chile is characterized by the use of a high density of reinforced concrete structural walls, in comparison with the practice in Mexico, where the combination of frames and a low density of structural walls is typical. For this reason, in this study for the case of reinforced concrete buildings in Mexico, based on the combination of frames and structural walls, the value equal to 10 s^{-1} is used for λ (Piedrahita and Rodriguez, 2021). When calculating the global distortion D_{rm} using Eq. (20) for reinforced concrete buildings in Mexico that are either solely based on frames or a combination of frames and structural walls, and applying Eq. (19) with a height h of 3.5 m and the previously mentioned values of λ, the stiffness indices *H/T* result in values of 28 m/s and 35 m/s, respectively. Furthermore, to illustrate the case of using a high density of structural walls, as occurs in Chilean practice, the case λ= 14, i.e. *H/T* =49 m/s, is also considered.

For the estimation of the maximum floor-to-floor distortion in regular frame-based buildings, d_{rm}, a possible lower limit of this parameter is considered to be given by (Cecen, 1979; Miranda, 1999; Piedrahita and Rodriguez, 2021):

$$d_{rm} = 1.5\, D_{rm} \qquad (21)$$

In a frame building with a weak first floor, which occurs in the construction practice in Mexico, the value of d_{rm} could be much higher than the value given by Eq. (21); these cases are not considered in this study, since it refers to regular structures.

In the case of regular buildings in Mexico, when frames and structural walls are combined, it is considered (Piedrahita and Rodriguez, 2021):

$$d_{rm} = 1.3\, D_{rm} \qquad (22)$$

The lower amplification of the interstory distortions in wall buildings compared to frame buildings is due to the typical modal shapes of these two different structures.

4.2 Design distortions in reinforced concrete buildings with different types of structures and distortions calculated for a record of accelerations. The case of the Miramontes station site in Mexico City

It has been shown, see Figs. 5 and 6, that the seismic demands recorded at the Miramontes station in the September 19, 2017 earthquake were, in certain period intervals, greater than the demands stipulated by NTCS (2004) and by NTCS 2017 at the site of the location of this station. This observation is congruent with the amount of damage, structural and nonstructural, observed in this earthquake in structures located on soils with comparable characteristics, particularly when considering the dominant period of the ground. Therefore, to illustrate the importance of the type of structural system used to limit damage or collapse in structures in earthquakes, this paper employs the record of S00E accelerations obtained at the Miramontes station in the earthquake of September 19, 2017, as well as the design spectral ordinates specified by the

NTCS 2017 for the site of this station.

The displacements obtained using the design spectra defined in Chapter 3 of the NTCS 2017 standards, when multiplied by QR, correspond to the S_d parameter in Eq. (20). The parameter R represents the over-resistance factor, and according to the NTCS 2017, for its calculation, the factor R_0 is considered equal to 1.75 for the case where Q = 2, and equal to 2.0 for the case where Q = 4. The factor k_1 used in the computation of R is equal to 1. The factor k_2, also used in the computation of R, is obtained from expression 3.5.2 of the NTCS 2017.

As mentioned above, the approximate computation procedure for the distortion d_{rm}, in the case of frame-based structures, uses the stiffness index H/T = 28 m/s. The results obtained with this procedure for the floor-to-floor distortion, d_{rm}, corresponding to the referred design spectra for the cases Q = 2 and Q = 4 are shown in Fig. 11, which are identified in this figure as the cases SASID, Q = 2 and SASID, Q = 4, with thick and thin dashed lines, respectively. Fig. 11 also shows the distortions d_{rm} resulting from the nonlinear analysis of frame-based structures, with the approximate procedure described, using the accelerations record S00E obtained at the Miramontes station in the 2017 earthquake, the value of the critical damping fraction ξ = 5%, and considering the cases of displacement ductilities, μ, equal to 2 and 4, which are shown with black and gray solid lines, as Duc = 2 and Duc = 4, respectively.

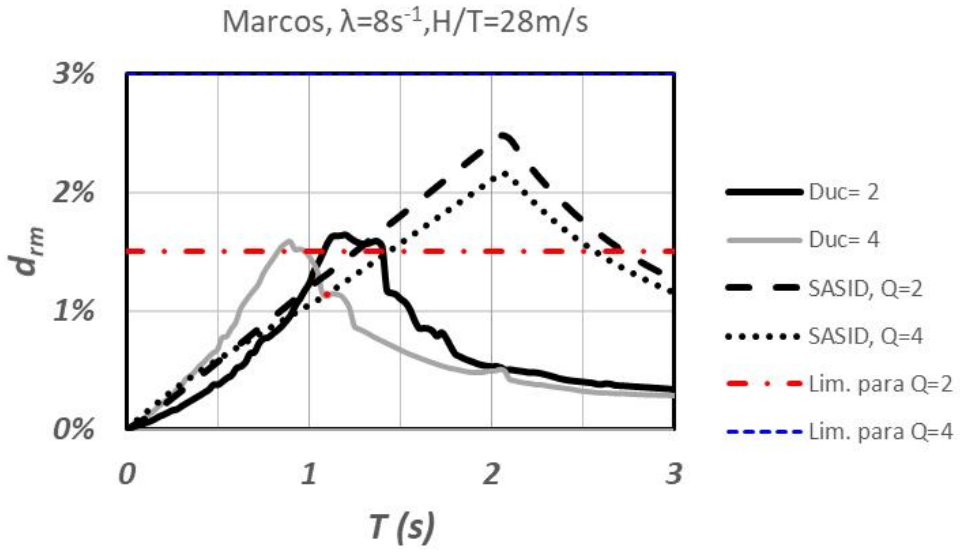

Figure 11. Spectral displacements in the inelastic interval obtained with the S00E accelerations record of the September 19, 2017 earthquake at Miramontes station for the cases of displacement ductilities equal to 2 and 4, and spectra obtained with NTCS 2017 and with SASID for the cases Q = 2 and Q = 4. Case frames H/T = 28 m/s.

The results in Fig. 11 indicate that in the wide period interval from 1.2 s to 2.7 s, frame-based buildings designed with NTCS 2017 and Q = 2 would have maximum interstory distortions greater than 1.5%, which is the distortion limit allowed by NTCS 2017 for frame-based buildings designed with Q = 2. This implies that in this period interval, it would not be possible to use buildings based on frames designed with Q = 2, and it would be necessary to use more rigid structures, for example, with structural walls, as shown in the following. In addition, the results in Fig. 11 show that in certain zones of periods less than 1.3 s, the demands of interstory distortions in frame-based buildings obtained from the nonlinear analysis with the S00E record of the Miramontes station, with displacement ductilities equal to 2 and 4, exceed the design demands stipulated by the NTCS 2017, as shown by the lines Duc = 2 and Duc= 4 in Fig. 11. Moreover, the demands computed with the nonlinear analysis employed and the Miramontes station records, at small period intervals, are even slightly higher than the maximum allowable distortion value of 1.5%, see continuous lines in Fig. 11.

Fig. 12 shows results of interstory distortions in buildings where frames and walls are combined, with a density of these corresponding to the stiffness index H/T = 35 m/s. This value, as mentioned, is found in the design practice in Mexico City, when reinforced concrete structural frames and walls are combined. As illustrated in Figure 12, within the period interval from 1 s to 3 s, the systems designed with a combination of walls and frames using the NTCS 2017 standard and Q = 2, exceed the distortion limit of 1% stipulated by this standard for this type of structure. This limit is represented by the thick dashed line identified as SASID, Q = 2. Additionally, Fig. 12 demonstrates that these structural systems designed with Q = 4 would meet the NTCS 2017 requirement of not exceeding the 2% limit for this type of structure. This limit is indicated by the thin dashed line identified as SASID, Q = 4. However, in seismic-resistant design practice in Mexico, it is uncommon to encounter designs that employ Q = 4 Furthermore, designing with large allowable distortions implies accepting greater potential damage to the structure. Therefore, in the case of designing with Q = 4, it is advisable to consider using even stiffer structures, as shown below.

Fig. 12 also shows that, in buildings with structural walls where H/T = 35 m/s, at small period intervals, the interstory distortion demands obtained from the nonlinear analysis with the S00E log of the Miramontes station, with displacement ductility equal to 2, are slightly greater than the maximum allowable distortion value of 1 %, as shown by the continuous lines Duc = 2 in Fig. 12.

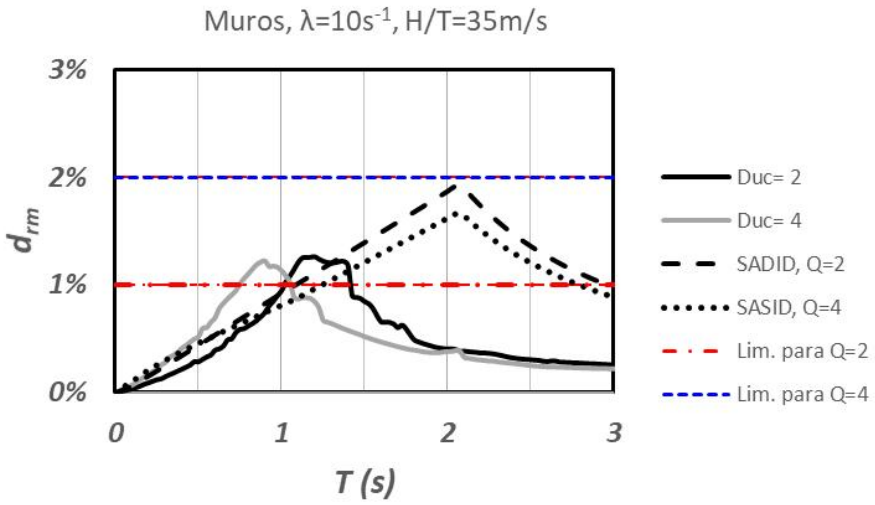

Figure 12. Spectral displacements in the inelastic interval obtained with the S00E accelerations record of the September 19, 2017 earthquake at Miramontes station for the ductility cases of displacements equal to 2 and 4, and spectra obtained with NTCS 2017 and with SASID for the cases Q = 2 and Q = 4. Case buildings with structural walls, H/T = 35 m/s.

Fig. 13 shows results from the use of reinforced concrete buildings with wall densities similar to those that would be found in Chilean practice. These results were obtained for the case of the stiffness index H/T = 49 m/s. Fig. 13 shows that, for this case, in a wide interval of periods, the values of the interstory distortion spectra, are less than the 1% distortion limit stipulated by NTCS 2017 for structures employing structural walls designed with Q = 2. For these structures, the distortions obtained with NTCS 2017 are greater than 1% and less than 1.4% in the period interval from 1.5 s to 2.5 s. For the case Q = 4, the distortions obtained with NTCS 2017 are less than the 2% distortion limit stipulated by NTCS 2017 for this type of structures. These distortions for the Q = 4 case are greater than 1% and less than 1.2% in a small interval of periods, from 1.7 s to 2.2 s. These results show the importance of the use of structural walls to significantly reduce the interstory distortion demands, and thus reduce the damage in buildings responding to earthquakes.

Fig. 13 also shows that, in buildings with structural walls where H/T = 49 m/s, the interstory distortion demands

obtained from the nonlinear analysis with the S00E register of the Miramontes station, with displacement ductilities equal to 2 and 4, are less than the maximum allowable distortion value of 1 %, as shown by the continuous lines Duc = 2 and Duc = 4 in Fig. 13.

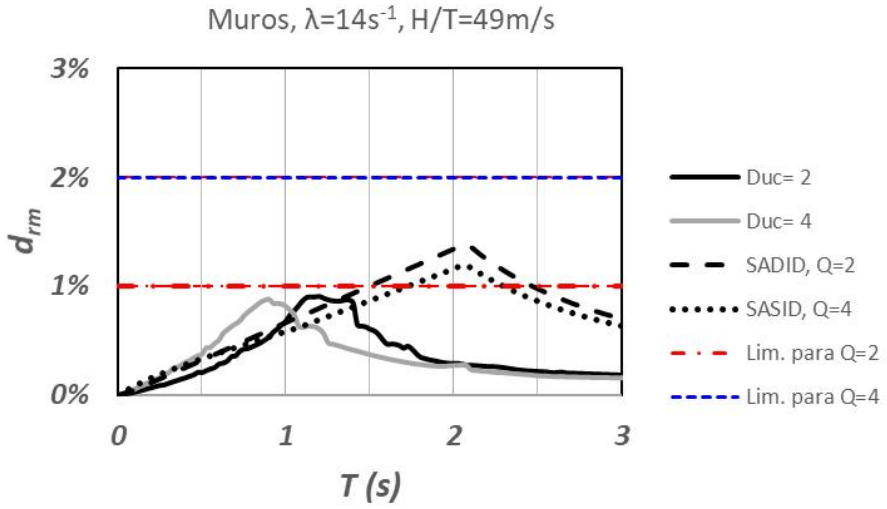

Figure 13. Spectral displacements in the inelastic interval obtained with the S00E accelerations record of the September 19, 2017 earthquake at Miramontes station for the ductility cases of displacements equal to 2 and 4, and spectra obtained with NTCS 2017 and with SASID for the cases Q = 2 and Q = 4. Case buildings with structural walls, H/T = 49 m/s.

5. Values of the Limiting Distortion γ_{max} Specified by NTCS 2017

The NTCS 2017 specifies limit values for the interstory distortion, γ_{max}, which depend on the ductility level of the structure. This standard stipulates three levels of ductility, which depend on the detailing, and are high, medium and low, which correspond to seismic behavior factors, Q, equal to 4, 3 and 2, respectively. In general, for concrete or steel structures, the higher the value of Q, the higher the value of limit distortion γ_{max}. For example, in the case of concrete structures, for systems formed by frames designed with values of Q equal to 2 and 4, the values of γ_{max} are equal to 0.015 and 0.03, respectively. For systems formed by concrete walls designed with Q values equal to 2 and 4, the γ_{max} values are equal to 0.01 and 0.02, respectively. These values of γ_{max} suggest that the expected interstory distortions in low ductility structures are smaller than those corresponding to high ductility structures, which is not necessarily the case, as shown in the following.

The results presented in Fig. 11 to 13 indicate that, in structures designed according to the NTCS 2017 standard, with Q values of 2 and 4, the interstory distortions observed for these Q values are not significantly different. This characteristic is explained in the following. For the collapse safety limit state, according to NTCS 2017, the maximum interstory distortions are obtained with the design spectrum defined in Chapter 3 of this standard, multiplied by QR, this procedure implies employing the elastic spectrum of unreduced accelerations, S_{aEl}, multiplied by Q/Q'. This conclusion can be reached by considering that the ordinate of the design spectrum defined in Chapter 3 of NTCS 2017 is equal to $S_{aEl}/(Q'R)$, which multiplied by QR leads to the value $S_{aEl}\ Q/Q'$. For this case, the spectral displacement S_d is obtained as:

$$S_d = \frac{1}{\omega^2}\ S_{aEl}\ \frac{Q}{Q'} \qquad (23)$$

Where ω is the circular frequency.

Fig. 14 shows results of applying Eq. (23) with the values of spectral accelerations obtained with SASID for the Miramontes station site, using the values of Q equal to 2 and 4. It can be shown that, in the case of these accelerations, in a wide interval of periods the values of Q and Q', for the cases of Q equal to 2 and 4, are not very different. This implies that according to Eq. (23), the values of S_d for these values of Q would not be very different either, which explains the results for S_d shown in Fig. 14. As shown in Eq. (20), the global distortion D_{rm}, and hence the interstory distortion, d_{rm}, see Eq. (21), for a type of earthquake-resisting structural system is mainly a function of S_d. Therefore, the little difference mentioned of the values of S_d in Fig. 14 for the cases Q = 2 and Q = 4, is also reflected in the calculated values of the interstory distortion d_{rm} shown in Figs. 11 to 13 for the different structural systems considered. These design demands obtained using the NTCS 2017 shown in these figures are not congruent with the values stipulated by the NTCS 2017 for the limit distortion γ_{max}. For example, for frame-based systems or with concrete walls designed with Q equal to 4, the stipulated value for γ_{max} is twice the value corresponding to the case of these systems designed with Q equal to 2. This characteristic is not in line with the distortion design requirements depicted in Figs. 11 to 13 for the cases where Q is equal to 2 and 4, respectively labeled as SASID, Q = 2 and SASID, Q = 4 in these figures. This is because the distortions shown in Figs. 11 to 13 do not exhibit significant differences as specified for γ_{max} in these respective cases.

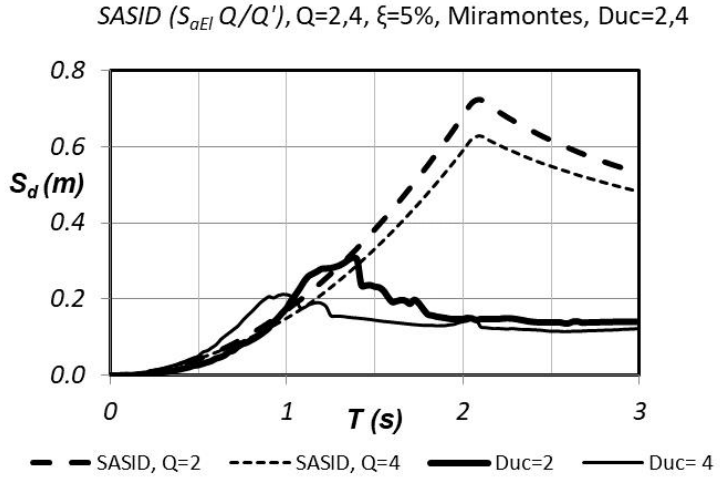

Figure 14. Spectral displacements obtained with the SASID program at the Miramontes station site for the cases Q = 2 and Q = 4. Spectral displacements of an oscillator responding to the S00E accelerations record of the September 19, 2017 earthquake at the Miramontes station for the cases of displacement ductilities equal to 2 and 4., ξ = 5%.

The notion that the expected interstory distortions in low ductility structures are smaller than those in high ductility structures, as indicated by the γ_{max} limits set by NTCS 2017 for these respective cases, is also inconsistent with the results of a nonlinear analysis conducted to compute interstory distortions in structures exhibiting varying degrees of displacement ductility and responding to an acceleration record obtained from non-rigid soil or rock, such as the S00E record from the Miramontes station (see Figs. 11 to 13). The reasons for this inconsistency are elaborated below. The results presented in Figs. 11 to 13 show that, for periods exceeding 1 s, the calculated interstory distortion values for structures with low ductility (identified in these figures as Duc = 2) are greater than those for the design case with high ductility (identified as Duc = 4). Conversely, only in the period range of less than 1 s, structures with high ductility exhibit higher distortion values than those with low ductility, as evident from Figs. 11 to 13. These characteristics of the response of these structures can be explained from the inspection of the creep resistance of the oscillator with nonlinear response shown in Fig. 6, which shows that for periods less than 1 s, the resistances of the structures with low ductility (Duc = 2) and those corresponding to high ductility (Duc = 4), have close values, and have the same value for $T = 0$. For periods longer than 1 s,

the resistances of structures with low ductility tend to be higher than those corresponding to the case of high ductility, see Fig. 6, which, for this period interval, implies higher values of d_{rm} in structures with low ductility with respect to those corresponding to structures with high ductility, see Figs. 11 to 13. These results of distortions of structures responding to a record of accelerations, as well as the distortions that would be obtained in structures designed with the NTCS 2017, indicate the need to review the values stipulated by these standards for the limit distortion γ_{max}.

6. Conclusions

In all the cases of the earthquakes in the world selected for this research, the seismic demands observed in these earthquakes exceeded the demands stipulated by building regulations in the respective earthquake locations. This shows the limitations of the probabilistic models used to define the seismic hazard and the consequent design earthquake.

This work shows possible uncertainties in the use of seismic analysis models of structures, related to discrepancies between the measured values, and the values of effective stiffness and modulus of elasticity of concrete that stipulate design standards for these analyses. Additionally, uncertainties that exist in the computation of the seismic response of irregular structures are discussed, as well as limitations of conventional modal seismic analysis.

The uncertainties in the values of the design seismic actions, the uncertainties in the results of the use of seismic analysis models of structures, the amplification of seismic demands in irregular buildings, as well as the limitations of conventional modal seismic analysis, suggest that it is not sufficient for structures to have the required lateral resistance required by the seismic design regulations, and that it is necessary for structures to have reserves of deformation capacity. These reserves would not be possible in structures designed with the seismic behavior factor Q = 2, a value commonly used in Mexico. This is due to the fact that in these structures the deformation capacity of their critical sections is low. It is important to consider the importance of transverse reinforcement in reinforced concrete elements to improve the deformation capacity of the critical sections of structural elements subjected to earthquakes. This implies that it is desirable that structures designed with Q = 2 should not be used in the lake area of Mexico City, nor in areas of high seismicity in the country, as is the case of the Pacific coast of Mexico.

This study employs approximate methods for the computation of interstory distortion demands in regular buildings with different structures subjected to seismic actions. Buildings with structural systems using only reinforced concrete frames, or systems with reinforced concrete structural walls, were considered. With these methods, demands of interstory distortions in buildings were calculated for the cases of seismic demands specified by the NTCS 2017 at the Miramontes station site. The results found show that, in a wide area of fundamental periods of frame-based buildings designed with Q = 2, the interstory distortions exceed the limit value specified by NTCS 2017 for these structures, which implies that the use of structural walls, in some cases with significant wall densities, is necessary to comply with this limit. These wall densities define the *H/T* stiffness ratio used in this work, and it has been shown that increasing values of this ratio allows reducing distortion demands in buildings subjected to earthquakes.

With these approximate procedures, nonlinear dynamic type analyses were performed for the computation of distortions in buildings responding to S00E acceleration records obtained at the Miramontes station in the earthquake of September 19, 2017, considering the cases of displacement ductilities equal to 2 and 4. It was found that, at small period intervals, these calculated distortion demands exceeded the distortion limits stipulated by the NTCS 2017 for the case of structural systems based only on frames, and for the case of systems with low density of structural walls (with stiffness index *H/T* =35 m/s).

This study highlights the importance of limiting the use of flexible structures, similar to frame based structural systems, which cannot only cause damage or collapse of so-called non structural elements in strong or even moderate

earthquakes, but also lead to the collapse of these structures, as occurred in the September 19, 1985 and 2017 earthquakes in Mexico City.

The values of the limiting interstory distortion, γ_{max}, specified by the NTCS 2017 suggest that the maximum interstory distortions expected in low ductility structures are lower than those corresponding to high ductility structures. This idea is not congruent with the results of this work, which shows that the maximum distortions that would be obtained in structures designed with the NTCS 2017 procedures, for the low and high ductility cases, are not very different. Nor is the referred idea congruent with the results of the nonlinear analysis for the computation of maximum distortions in structures with different structural systems, when they respond to a record of accelerations obtained in soft soil in the earthquake of September 19, 2017. As shown in this work, in these cases, it is even observed that it is possible that structures with low ductility, have higher values of interstory distortions than those corresponding to the cases of structures with high ductility. These results suggest the revision of the allowable values of the interstory distortions stipulated by the NTCS 2017.

Conflicts of Interest

The author declares no conflicts of interest regarding the publication of this paper.

References

[1] ACI 318-19 (2019). "Building Code Requirement for Reinforced Concrete". American Concrete Institute.

[2] ACI-363 (1992). "Report on High-strength Concrete". American Concrete Institute Committee 363.

[3] ASC/SEI 7-10, (2016), "Minimum Design Loads for Buildings and Other Structures", American Society of Civil Engineers. Estados Unidos.

[4] Bradley B., Quigley M., Van Dissen R. Litchfiled N., (2014) "Ground Motion and Seismic Source Aspects of the Canterbury Earthquake Sequence", *Earthquake Spectra*, 30(1): 1-15.

[5] Cecen, H. (1979), "Response of Ten Story, Reinforced Concrete Model Frames to Simulated Earthquakes", Tesis para obtener el grado de Doctor en la Escuela de Graduados de Ingeniería Civil de la University of Illinois at Urbana-Champaign, Estados Unidos.

[6] Diario Oficial (2011), Decreto N61, Diario Oficial de la República de Chile, 13 de diciembre 2011.

[7] EERI (2011), "The M 6.3 Christchurch, New Zealand, Earthquake of February 22, 2011", EERI Special Earthquake Report", 1-16

[8] Elwood, K., y M. Eberhard. (2009). "Effective stiffness of reinforced concrete columns." *ACI Structural Journal*, 106(4): 476-484.

[9] Instituto Nacional de Normalizacion (1996), "Norma Chilena Oficial. Diseño Sísmico de edificios". NCh433.Of 1996. Chile

[10] Lagos, R., Kupper, M., Lindenberg, J., Bonelli, P., Saragoni, R., Gueldelman, T., Massone, L., Boroschek, R., and Yanez, F., (2012). Seismic Performance of High-Rise Concrete Buildings in Chile, *International Journal of High-rise Buildings*, 1(3): 181-194.

[11] Massone L., Bonelli P., Lagos R., Luders C., Moehle J. y Wallace J. (2012), "Seismic Design and Construction Practices for RC Structural Wall Buildings", *Earthquake Spectra*, 28(S1): S245-S256.

[12] Miranda, E. (1999). "Approximate Seismic Lateral Deformation Demands in Multistory Buildings", *Journal of Structural Engineering*, 125(4): 417-425.

[13] Normas Técnicas Complementarias por Sismo (2004). Gaceta Oficial del Distrito Federal.

[14] Normas Técnicas Complementarias por Sismo (2017). Gaceta Oficial de la Ciudad de México.

[15] Normas Técnicas Complementarias para Diseño y Construcción de Estructuras de Concreto, (2017), Gaceta Oficial de la Ciudad de México.

[16] Piedrahita, I. y Rodriguez, M. (2021), Ejemplo 13, en "Ejemplos de diseño de acuerdo con las Normas Técnicas Complementarias para Diseño por Sismo 2017/2020", SMIE, SMIS, ISBN 978-607-95994-3-0

[17] Pujol, S., y Rodriguez, M.E. (2019), "Evaluación del comportamiento de muros no estructurales en edificios de la Ciudad de México en el terremoto del 19 de septiembre 2017", *Revista de Ingenieria Sísmic*a, 101: 53-66.

[18] RCDF (1976), "Reglamento de Construcciones para el DF". Diario Oficial de la Federación.

[19] Rodríguez, M, Restrepo, JI y Carr, AJ (2002). "Earthquake induced floor horizontal accelerations in buildings", *Earthquake Engineering & Structural Dynamics*, 31: 693-718.

[20] Rodríguez M.E. y Restrepo J., (2012), "Practica y diseño sísmico de edificios en México. Cambios necesarios", *Revista de Ingenieria Sísmica*, 86: 89-112.

[21] Rodriguez, M. (2016) "Una revisión crítica de la práctica de diseño por sismo de estructuras en México", *Revista de Ingenieria Sismica*, 94: 27-48.

[22] Rodriguez M. E. (2018), "Damage Index for Different Structural Systems Subjected to Recorded Earthquake Ground Motions", *Earthquake Spectra*, 34(2): 773-793.

[23] Rodriguez, M.E. (2020). "The Interpretation of Cumulative Damage from the Building Response Observed in Mexico City During the September 19, 2017 Earthquake", *Earthquake Spectra*, 36(2): 199-212. DOI: 10.1177/8755293020971307.

[24] Rodelo, R., Rodriguez, M., y Restrepo, J. (2020), "Parámetros relevantes de la curva esfuerzo-deformación de concretos no confinados producidos en México", *Revista de Ingeniería Sísmica*, 103: 18-36.

[25] Restrepo J. y Rodriguez, M. (2021) "Stiffness Modifiers to Support the Seismic Design of Reinforced Concrete Rectangular Columns", *Journal of Structural Engineering*, ASCE, Vol 147, No 10. DOI: 10.1061/(ASCE)ST.1943-541X.0003123.

[26] Saiidi M. y Sozen M. (1981), "Simple Nonlinear Analysis of RC Structures", *Journal of Structural Engineering*, ASCE, Vol 197, 937-952.

[27] Sharooz, B., y Moehle, J. (1990), "Seismic Response and Design of Setback Buildings", *Journal of Structural Engineering*, Vol. 116, No. 5, 1423-1439.

[28] Standards New Zealand (2004), NZS 1170.5:2004, "New Zealand Standard. Structural design actions. Part 5: Earthquake Actions-New Zealand".

[29] Standards New Zealand (2006), NZS 3101, "Concrete Structure Standard, Part 1: The Design of Concrete Structures. Part 2: Commentary on the Design of Concrete Structures".